JOURNAL OF CATALYSIS 118, 238–254 (1989)

Characterization of Silica-Supported Ruthenium Catalysts by Hydrogen Chemisorption and Nuclear Magnetic Resonance of Adsorbed Hydrogen

X. WU,* B. C. GERSTEIN,† AND T. S. KING*,[1]

*Department of Chemical Engineering, 231 Sweeney Hall, and †Department of Chemistry, 219 Spedding Hall, Iowa State University, Ames Laboratory, Institute for Physical Research and Technology, Ames, Iowa 50011

Received December 16, 1988; revised March 13, 1989

Adsorbed hydrogen on four silica-supported ruthenium catalysts was measured quantitatively by proton magnetic resonance (PMR). The PMR technique revealed two distinct adsorbed states of hydrogen on the metal: reversible and irreversible. The results from PMR and those from conventional hydrogen chemisorption measurements were compared directly. The observed discrepancy between the PMR and volumetric techniques in the case of total adsorption is attributed to spillover of reversibly adsorbed hydrogen from ruthenium onto the silica support. Good agreement was obtained between the two techniques in the case of irreversible adsorption. The relatively narrow line of PMR spectra on the reversibly adsorbed hydrogen indicates rapid motion for this state of hydrogen on ruthenium surfaces. The variation of spectral lineshift and of the spin–lattice relaxation times for the adsorbed hydrogen with ruthenium particle size suggests a stronger interaction between the adsorbed hydrogen and defect-like ruthenium adsorption sites. The results from PMR intensity measurements also suggest that the reversibly adsorbed hydrogen is at least in part associated with the defect-like ruthenium adsorption sites.

INTRODUCTION

Dissociative adsorption of hydrogen on Group VIII transition metal surfaces is well known and is the basis for the volumetric method of selective hydrogen chemisorption on these supported metal catalysts. This technique has been used to measure the ruthenium dispersion (fraction of ruthenium atoms at the metal surface) in Ru/SiO_2 (*1–4*), Ru/Al_2O_3 (*5, 6*), and Ru/Y (*6–8*) catalysts. The basic assumptions involved in obtaining the dispersion by this method include (i) a specific stoichiometry between the absorbed hydrogen atoms and the ruthenium atoms at the surface, and (ii) no hydrogen spillover from ruthenium onto the support. Using total hydrogen adsorption, Dalla Betta (*1*), Kubicka (*2*), Taylor (*5*), and Goodwin (*6*) estimated the stoichiometric ratio $H/Ru_{(s)}$ to be in the range of 1.1 to 1.5, although $H/Ru_{(s)} = 1.0$ was recommended by some of these researchers.

However, there are indications of two adsorbed states of hydrogen on ruthenium powder (*9*), Ru/SiO_2 (*10*), and Ru/Y (*7*) catalysts, namely, the strongly (or irreversibly) adsorbed hydrogen and the weakly (or reversibly) adsorbed hydrogen. The irreversible adsorption may be attributed to strong chemisorption of hydrogen on ruthenium. The reversibly adsorbed hydrogen is known to be readily removed by evacuation at ambient temperature, and it may be attributed to either multiple adsorption of hydrogen on ruthenium alone or both multiple adsorption and hydrogen spillover onto the support. But there is no convincing evidence in the literature to support or exclude the possibility of hydrogen spillover in supported ruthenium catalysts. Some evidence of hydrogen spillover onto the support at ambient temperature in silica- and zeolite-supported platinum catalysts has been

[1] To whom correspondence should be addressed.

0021-9517/89 $3.00

found by hydrogen chemisorption measurements (*11, 12*), which showed an enhanced adsorption of hydrogen (H/Pt > 1.0) in these catalysts. If this is true, hydrogen spillover could occur in silica-supported ruthenium catalysts as well.

There is an additional complication in characterizing supported ruthenium catalysts when $RuCl_3 \cdot nH_2O$ is used as a precursor in preparing the catalysts. Recent studies (*13–16*) showed that chlorine cannot be effectively removed from the surface of ruthenium particles at usual reduction temperatures (573–773 K) and that it inhibits adsorption of hydrogen on ruthenium. Since chlorine-contaminated ruthenium catalysts were used in most of the previous studies (*1–5*), the results obtained from these catalysts may be questionable and are worth reexamining.

Nuclear magnetic resonance (NMR) of hydrogen atoms or proton magnetic resonance (PMR) has been applied to measure the resonance linewidth and lineshift of hydrogen adsorbed on silica- and alumina-supported platinum catalysts (*17–19*). Also PMR has been applied to measure the lineshift of hydrogen adsorbed on ruthenium in Ru/SiO_2 catalysts (*19, 20*), although the lineshift may have been influenced by the chlorine impurity. In fact, marked changes in the lineshift of the hydrogen adsorbed on ruthenium due to the chlorine residue have been observed (*21*). Also, previous intensity measurements (*19*) on the upfield peak, which corresponds to resonance of the hydrogen adsorbed on ruthenium, could account for only 70% of the total adsorbed hydrogen by volumetric measurements. The discrepancy may be due to inherent experimental errors and/or hydrogen spillover onto the silica support.

The objective of the present study was to examine the validity of hydrogen chemisorption in determining ruthenium dispersion on clean Ru/SiO_2 catalysts by the technique of proton magnetic resonance and to investigate the nature of the reversibly adsorbed hydrogen in these catalysts. PMR offers a great advantage in discerning between the reversibly adsorbed hydrogen on ruthenium and the spiltover hydrogen on the silica support.

METHODS

Catalyst Preparation

All catalysts were prepared by incipient wetness impregnation of a ruthenium impregnating solution with a dried Cab-O-Sil HS5 (300 m^2/g BET surface area) silica support. The impregnating solution was prepared by dissolving an appropriate amount of $Ru(NO)(NO_3)_3$ salt (AESAR) in distilled water. Approximately 2.2 ml of impregnating solution per gram of support was needed to bring about incipient wetness. The slurries obtained after impregnation were dried for 24 h at room temperature and 4 h in air at 383 K. Catalysts with ruthenium loadings of 1, 4, 8, and 12% by total weight of ruthenium metal plus dry support were prepared for the present study.

Adsorption Apparatus

The adsorption apparatus used in this study was a multiport high-vacuum Pyrex glass manifold with a volume of 127.3 cm^3 in connection with a turbo-molecular pump (Balzers, Model TPH050) backed by a forepump trap and a two-stage mechanical pump. High-vacuum greaseless, bakeable stopcocks (Ace Glass) with Teflon plugs and FETFE O-ring seals were employed to manipulate gas storage, dosage, or both and to minimize hydrocarbon impurities in the manifold. The manifold was capable of a vacuum better than 10^{-7} Torr (1 Torr = 133.3 Pa) after bakeout. Pressures below 10^{-2} Torr were monitored by a cold cathode gauge (Varian Model 860A). Pressures from 10^{-2} to 10^3 Torr were measured by two Baratron absolute pressure gauges (MKS Instruments).

Catalyst samples were held in a Pyrex cell by a coarse frit with an average pore diameter of 35 μm. A small furnace was used to heat the cell. The temperature of

the furnace was controlled by a temperature controller (Omega Engineering) to within ±1 K.

Catalyst Reduction and Adsorption

All catalyst samples were treated inside the Pyrex cell. Approximately 1 g of sample was loaded into the cell, which was then attached to one of the sample ports of the manifold. While helium was allowed to flow through the cell, the temperature of the furnace surrounding the cell was raised to 423 K. Then helium was replaced by hydrogen gas at a flow rate of 50 cm^3/min, and reduction proceeded for 1 h at that temperature before it was raised at 10 K/min to 723 K. Further reduction was carried out for an additional 2 h at 723 K. Helium (99.999%) and hydrogen (99.8%) (Liquid Air Co.) were used as received. After reduction, a 2-h evacuation period at 723 K was followed to remove traces of water and surface hydrogen.

Hydrogen used for adsorption was purified by passing it through a catalytic hydrogen purifier (Engelhard Deoxo) in series with a gas purifier with Drierite and 5-Å molecular sieve (Alltech) to remove traces of oxygen and moisture. Hydrogen adsorption experiments were performed at room temperature (294 K). The total hydrogen adsorption isotherm was measured in the pressure range 0–30 Torr. The reversible hydrogen adsorption isotherm was collected under the same conditions after a 10-min evacuation to 10^{-6} Torr following the total adsorption. The irreversible uptake was obtained by taking the difference between the extrapolated values of these two isotherms at zero pressure. Equilibration times of 4 h and 1 h were used for the first dose and for subsequent doses, respectively.

NMR Sample Treatment

A specially designed needle-bellows assembly, which was made of stainless steel, was used for direct reduction of a catalyst sample in flowing hydrogen inside a 5-mm NMR tube. The syringe needle (18 gauge) was capable of moving vertically by more than 6 cm through adjustable compression and extension of the bellows. Vacuum-tight connections were made between the NMR tube and the needle-bellows assembly and also between the assembly and the manifold. In addition, a small cylindrical furnace provided heating around the NMR tube and the temperature of the furnace was controlled to better than ±1 K.

With helium gas flowing through the needle, the needle was lowered down to the bottom of the NMR tube, which contained approximately 60 mg of catalyst sample. The reduction procedure was the same as previously described, with a hydrogen flow rate of 15 cm^3/min. After reduction, the needle was lifted out of the sample, and evacuation proceeded for 2 h at the reduction temperature before the sample was cooled to ambient temperature. Up to four samples could be reduced simultaneously. Then purified hydrogen was dosed through the needle to each sample separately and allowed to equilibrate for 4 h. The samples were then immersed in a water bath and the NMR tube was sealed off with a microtorch. Sample weights were measured after the NMR tubes were sealed.

For the deuterium exchange experiment, deuterium gas (Linde, 99.5%) instead of hydrogen was dosed to a ruthenium catalyst sample in an NMR tube immersed in liquid nitrogen. The NMR tube was sealed and the sample was temporarily stored in liquid nitrogen to inhibit the exchange until the sample was brought to room temperature at the onset of the exchange experiment.

NMR Experiments

The home-built NMR spectrometer (*22*) used for the present study was operated at 220 MHz for proton resonance. A proton-free probe with a doubly wound coil was used for all the NMR measurements. The probe quality factor Q was set at 100 for sufficient sensitivity and low ringdown time. A detailed description of the spec-

trometer's receiving system was given elsewhere (*20*).

The spectrometer was capable of detecting 10^{17} protons, while the number of hydrogen atoms adsorbed on ruthenium in a typical catalyst sample was around 5×10^{18}. The recycle time between 90° pulses was set between 0.2 and 0.3 s to suppress selectively the strong intensity of the peak corresponding to protons in the silanol group that have a relatively long spin-lattice relaxation time T_1 (on the order of seconds). The recycle rate given above avoids T_1 saturation of the peak corresponding to hydrogen adsorbed on ruthenium. The total number of scans for data acquisition on each sample was 10,000 unless noted otherwise. The inversion recovery pulse sequence (180°–τ–90°) was applied to measure the spin–lattice relaxation times of the silanol protons (in the time domain) and the hydrogen adsorbed on ruthenium (in the frequency domain). A pure water sample was used as the reference standard for the observed lineshifts. For the purpose of intensity measurements, the water sample was doped with $FeCl_3$ to yield a resonance of a comparable linewidth with the observed resonances. In addition, the doped water was sealed in a capillary tube with the same length as the catalyst sample in the NMR tube to offset errors due to B_1 inhomogeneity in the coil. All NMR measurements were done at ambient temperature (294 ± 1 K).

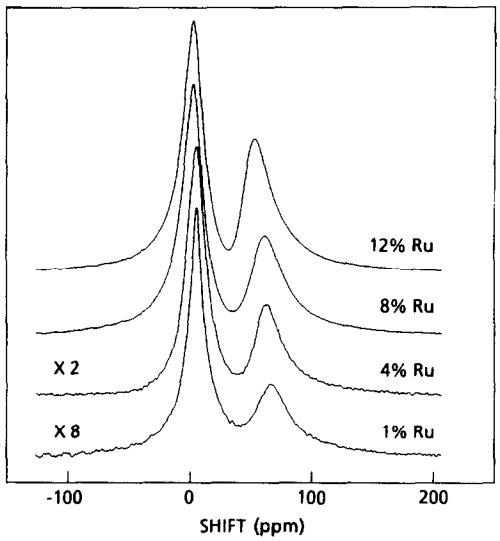

FIG. 1. PMR spectra of adsorbed hydrogen on Ru/SiO_2 catalysts. All catalyst samples are under 5 Torr hydrogen. Ruthenium weight loadings are as indicated. Water is used as reference for the lineshift.

RESULTS

PMR spectra of 1, 4, 8, and 12% ruthenium catalyst samples under 5 Torr hydrogen are shown in Fig. 1. As can be seen, two well-resolved resonance lines are clearly displayed in all spectra. The peak near the reference shift is designated the downfield peak and the peak on the right-hand side the upfield peak. The downfield peak is assigned to the terminal silanol protons (Si–OH) in the silica support since spectra for samples of these catalysts with no gaseous hydrogen added and a sample of silica under 5 Torr hydrogen all display only this peak. Note that the lineshift of the downfield peak moves from 5 to 3 ppm and the linewidth (full width at half-maximum) increases from 3.3 to 4.5 kHz as the ruthenium loading increases. The upfield peak has been assigned to hydrogen adsorbed on ruthenium (*19, 20*). The linewidth of the upfield peak decreases from 7.5 to 5.9 kHz with an increase in the ruthenium loading. There is also a noticeable change in the lineshift of the upfield peak toward downfield. Lineshift data for the upfield peak are shown later.

The downfield peak is symmetric and can be well fitted by a Lorentzian line. The upfield peak is asymmetric, especially for high ruthenium loadings. The area under the upfield resonance line can be obtained precisely by integrating the spectrum from which the downfield peak has been subtracted. The upfield peak location is calculated by the first moment of the subtracted spectrum.

The total hydrogen adsorption isotherms measured by both the volumetric technique

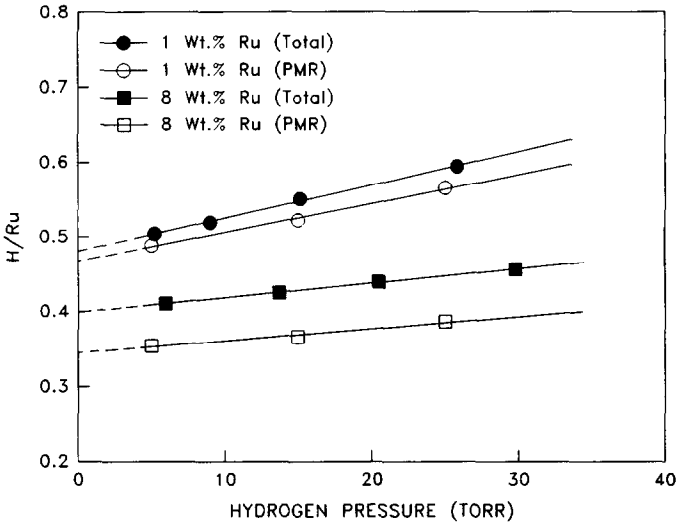

FIG. 2. Total hydrogen adsorption isotherms measured by both the volumetric technique and PMR on 1 and 8% Ru/SiO_2 catalysts at 294 K. The dashed lines represent extrapolation of the isotherms to zero hydrogen pressure.

and PMR for 1 and 8% ruthenium catalysts are shown in Fig. 2. For the PMR measurements, all data points are obtained from the upfield peak intensity only. All isotherms are extrapolated to zero hydrogen pressure to obtain the values for the H/Ru ratio. In both cases, the H/Ru value measured by total hydrogen adsorption is greater than that measured by PMR. In fact, this is true for all the catalysts, as will be shown.

In the hydrogen pressure range 5 to 30 Torr, the slope of the total adsorption isotherm is slightly greater than that of the PMR isotherm. The difference may be due in part to physisorbed hydrogen on SiO_2. However, the amount of physisorbed hydrogen on pure SiO_2 in this pressure range is less than 1% of the total hydrogen uptake on a catalyst sample. Extrapolation of the isotherm measured on SiO_2 yields zero hydrogen uptake, indicating that physisorbed hydrogen on SiO_2 makes no contribution to the measured H/Ru values.

The irreversible hydrogen uptake is the difference between the total hydrogen uptake and the reversible hydrogen uptake. The irreversible hydrogen adsorption isotherms for 1 and 8% ruthenium catalysts, which are derived from the corresponding total and reversible isotherms, are shown in Fig. 3. The values for irreversible hydrogen measured by PMR are also shown in the same figure for comparison. For PMR measurements, all samples were evacuated to 10^{-6} Torr for 10 min after they were equilibrated with 5 Torr hydrogen and only the intensity of the upfield peak, which corresponds to the irreversibly adsorbed hydrogen on ruthenium, was measured.

For both the 1% and the 8% ruthenium catalyst, portions of the irreversible isotherms obtained by the volumetric technique at hydrogen pressures below about 3 Torr probably do not represent the true equilibrium since adsorption at these low pressures require much longer time to reach equilibrium. Portions of the isotherms at hydrogen pressures beyond 3 Torr are nearly horizontal. This may be interpreted as formation of a complete monolayer of strongly chemisorbed hydrogen on ruthenium. The horizontal portions of the isotherms are extrapolated to zero pressure to obtain values of the H/Ru ratio. As can

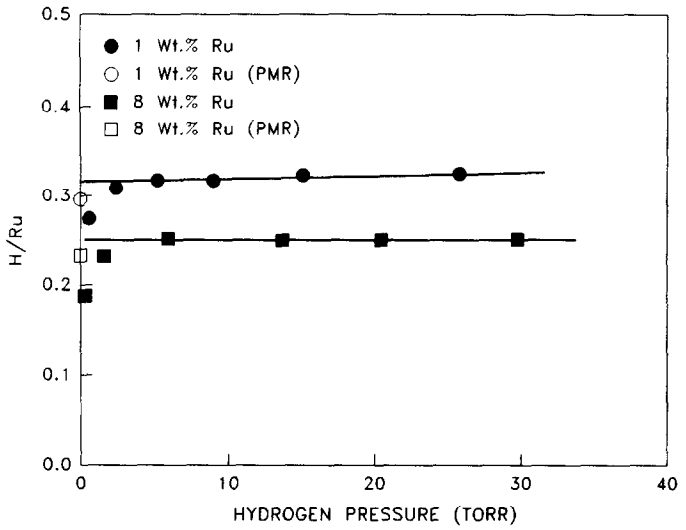

FIG. 3. Irreversible hydrogen adsorption isotherms obtained by the difference between the total and the reversible hydrogen adsorption isotherms on 1 and 8% Ru/SiO_2 catalysts at 294 K. The horizontal portion of the isotherms is extrapolated to zero hydrogen pressure. The amount of irreversibly adsorbed hydrogen on ruthenium measured by PMR is also shown for comparison.

be seen, the results from the PMR measurements are close to those from the volumetric measurements.

The total and irreversible H/Ru values measured by both techniques on all four ruthenium catalysts are shown in Fig. 4. The agreement between the two techniques is good for the irreversible hydrogen. However, noticeable discrepancies are observed for the total hydrogen adsorption, espe-

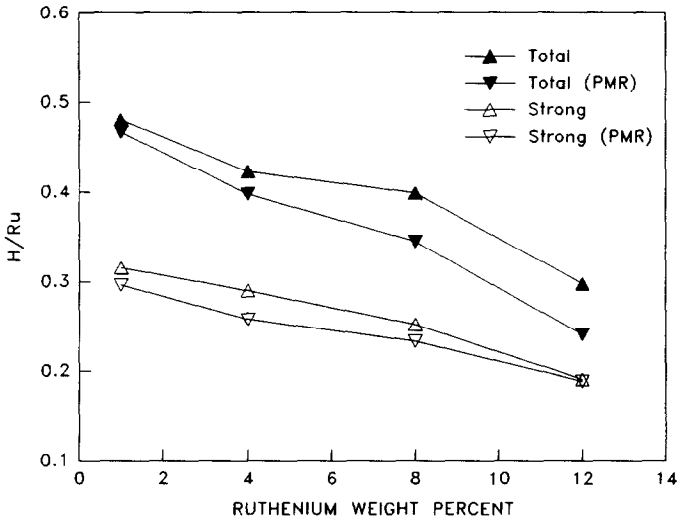

FIG. 4. The H/Ru ratios for both the total and the irreversible adsorption of hydrogen with variation in the ruthenium loading. Results from measurements by both the volumetric technique and PMR are shown for comparison.

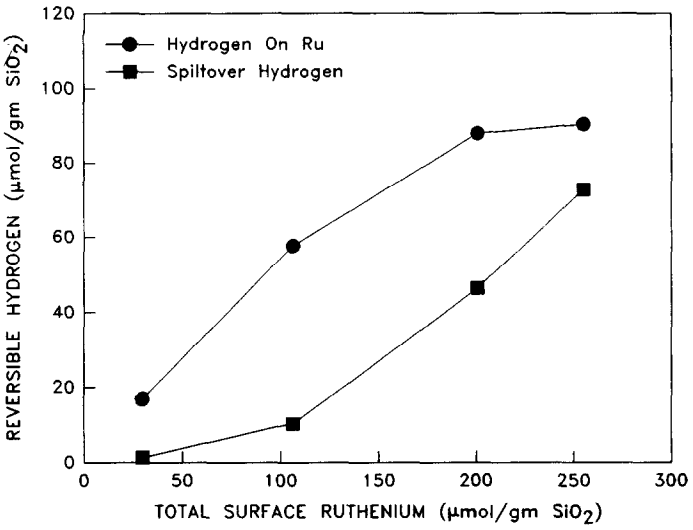

FIG. 5. Correlation among the reversible hydrogen on ruthenium (circles), the spiltover hydrogen (squares), and surface ruthenium. The total amounts of these two states of hydrogen are plotted as a function of the total amount of ruthenium at the surface.

cially for catalysts with high ruthenium loadings. One may argue that the discrepancies are only due to experimental errors. However, for high ruthenium loadings both the total amount of hydrogen adsorption and the PMR signal intensity are higher, which should lead to smaller experimental errors. A reasonable explanation is that hydrogen spillover from ruthenium onto the silica support is the cause for the observed discrepancies. This point will be discussed in more detail later.

The correlations between the total amount of reversible hydrogen on ruthenium and the total amount of surface ruthenium and between the total amount of spiltover hydrogen and the total amount of surface ruthenium are illustrated in Fig. 5, where 1 g of SiO_2 is used as the common basis. The amount of reversible hydrogen on ruthenium was computed from the difference between the H/Ru ratio for the total hydrogen and that for the irreversible hydrogen measured by PMR. The amount of spiltover hydrogen was obtained by taking the difference between the total H/Ru ratio measured by hydrogen chemisorption and that measured by PMR. The amount of surface ruthenium was calculated from the dispersion obtained from the H/Ru value for the irreversible hydrogen determined by PMR (see Fig. 4), assuming one irreversibly adsorbed hydrogen atom for every surface ruthenium atom, i.e., $H/Ru_{(s)} = 1$. As shown in the plot, both the total amount of reversible hydrogen on ruthenium and that of spiltover hydrogen increase with the increasing total amount of surface ruthenium.

Figure 6 shows the spectra for the irreversibly adsorbed hydrogen on ruthenium for both the 1% and the 8% ruthenium catalyst. The dotted resonance lines drawn above the upfield peaks are portions of the spectra corresponding to the same ruthenium catalyst under 5 Torr hydrogen pressure (which have been shown in Fig. 1). Since there is no significant change in the position of the upfield peak under these two conditions of hydrogen adsorption, it is appropriate to subtract one spectrum from the other to obtain the spectral features of the reversibly adsorbed hydrogen. The difference spectra between a sample under 5 Torr hydrogen and that under vacuum after

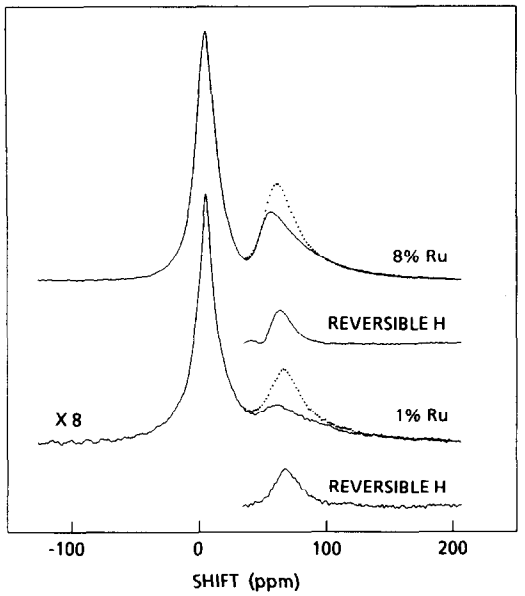

FIG. 6. Spectra of 5 Torr hydrogen, irreversibly adsorbed hydrogen, and reversibly adsorbed hydrogen on ruthenium for 1 and 8% Ru/SiO_2 catalysts. The spectra under 5 Torr hydrogen are shown as dotted lines. The spectra of reversible hydrogen, which are the difference spectra between 5 Torr hydrogen and irreversible hydrogen, are shown underneath the composite spectra.

hydrogen adsorption are shown in Fig. 6 underneath the composite spectra as the spectra for the reversibly adsorbed hydrogen on ruthenium.

Spectra shown in Fig. 6 clearly indicate that there are two adsorbed states of hydrogen on ruthenium, the irreversible hydrogen and the reversible hydrogen. The irreversibly adsorbed hydrogen displays an asymmetric resonance lineshape, while the reversibly adsorbed hydrogen has a relatively symmetric lineshape. The linewidths for the irreversible hydrogen are 8.7 and 11.8 kHz, and those for the reversible hydrogen are 3.8 and 5.6 kHz for the 8 and 1% ruthenium catalysts, respectively. Also, the resonance lineshifts of the reversible hydrogen are farther upfield than those of the irreversible hydrogen. The differences in lineshape, linewidth, and lineshift imply that these two adsorbed states of hydrogen are experiencing different environments on the surface of ruthenium particles. This is the first time the irreversibly adsorbed hydrogen and the reversibly adsorbed hydrogen on the surface of ruthenium particles are identified separately by means of proton magnetic resonance.

Shifts of the first moment of the upfield peak for 5 Torr hydrogen, the irreversible hydrogen, and the reversible hydrogen on ruthenium are shown in Fig. 7 as functions of the ruthenium loading. Obviously, a decreasing trend with increasing ruthenium loading is present for all the lineshifts. In all cases the lineshifts for the reversible hydrogen are farther upfield than those for the irreversible hydrogen. The difference in the lineshifts of these two adsorbed states of hydrogen decreases with increasing ruthenium loading.

Note that lineshifts reported in the present study are farther upfield than those reported in previous studies (*19, 20*) on ruthenium catalysts of similar metal loadings and under similar experimental conditions, even when the shifts of different reference standards are taken into account. We believe that such a disagreement is caused by residual chlorine on the surface of ruthenium particles in catalysts used in previous studies. Preliminary results (*21*) indicate that chlorine on the surface of ruthenium particles tends to move the upfield peak toward downfield.

The upfield peak shifts and spin-lattice relaxation times as functions of the hydrogen pressure for both the hydrogen adsorbed on ruthenium and the silanol proton are listed in Table 1. The lineshift of the upfield peak varies only slightly as the hydrogen pressure increases from 5 to 60 Torr. The small variation may be due to saturation of the ruthenium surface by the reversibly adsorbed hydrogen or exchange between this adsorbed state of hydrogen with hydrogen in the gas phase. This result agrees with observations by Sheng and Gay (*19*) that showed lack of variation of the upfield peak position with hydrogen cover-

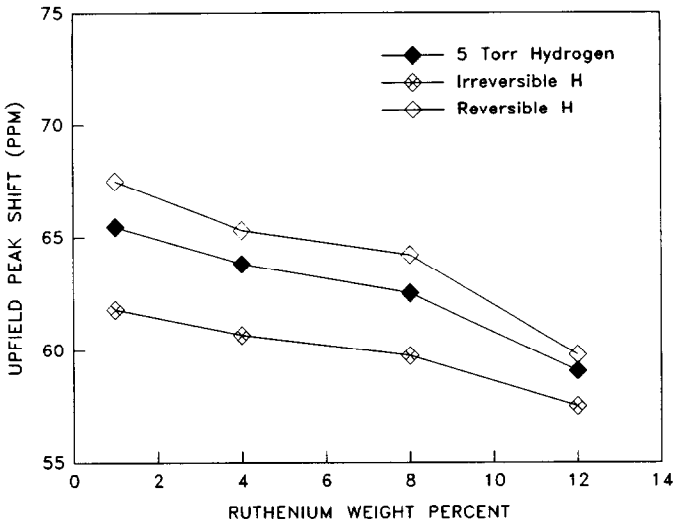

FIG. 7. Variation of the upfield resonance shift with the ruthenium loading. Shifts corresponding to 5 Torr hydrogen, irreversible hydrogen, and reversible hydrogen are shown.

age in Ru/SiO_2. Note that considerable variation of the upfield peak position with hydrogen pressure does occur in other systems such as supported Rh catalysts. A trend toward the upfield direction in the resonance position of the adsorbed hydrogen with increasing hydrogen coverage was reported for Rh/SiO_2 catalysts (*19*). On Rh/TiO_2 catalysts, the resonance of the adsorbed hydrogen shifts downfield with increasing hydrogen pressure (*23*). The discrepancy associated with the rhodium catalysts may be attributed to many factors such as residual chlorine on the metal surface, possible metal–support interaction, and varied rates of exchange between the reversibly bound hydrogen on the metal and the hydroxyl protons in the supports or hydrogen in the gas phase. These complications are absent for the Ru/SiO_2 catalysts prepared for the present study.

The effect of pressure on the spin–lattice relaxation times associated with the upfield and downfield peaks is also given in Table 1. As listed in the first two entries in Table 1, the spin–lattice relaxation time of the irreversibly adsorbed hydrogen on ruthenium is longer than that of the reversibly adsorbed hydrogen, considering the fact that the observed value of T_1 on the sample under 5 Torr of hydrogen is the combined relaxation effect from both the irreversible and the reversible hydrogen. Further increase in hydrogen pressure has little effect on T_1 of the hydrogen adsorbed on ruthenium. However, there is a marked decrease in the spin–lattice relaxation time of the silanol proton when both the ruthenium and the hydrogen are introduced to the silica

TABLE 1

Effects of Hydrogen Pressure on a 4% Ru/SiO_2 Catalyst

Hydrogen pressure (Torr)	Upfield peak shift (ppm)	Spin–lattice relaxation time T_1(s)	
		Upfield peak	Downfield peak[a]
0[b]	61	0.026	5.4
5	64	0.021	3.2
30	62	0.018	2.8
60	61	0.018	2.4

[a] The spin–lattice relaxation time of the silanol proton in a pure SiO_2 sample was 31.6 s and that in a 4% Ru/SiO_2 sample under vacuum (not hydrogen dosed) was 16.9 s.

[b] The catalyst sample was outgassed to 10^{-6} Torr for 10 min after adsorption of hydrogen.

support. A T_1 of 31.6 s was observed for protons in the silanol group in a pure silica sample. There was no significant change of this value when the pure silica was under 30 Torr of hydrogen gas. For a sample of 4% Ru/SiO_2 that has been reduced, outgassed, and sealed under vacuum, T_1 of the silanol group decreased to 16.9 s. We attribute this decrease to additional relaxation effects caused by ruthenium, to trace amounts of iron impurities that are associated with the ruthenium, or both. A significant decrease in the silanol group T_1 was observed when hydrogen gas was dosed onto the catalyst. Evacuation after hydrogen dosage resulted in only a small increase in the silanol group T_1, but it is still much lower compared to the catalyst sample without hydrogen dosage.

Using an average area of 0.0817 nm^2 per surface ruthenium atom (*1*), we calculated the total ruthenium surface areas. The average ruthenium particles sizes, d, were calculated by use of the relationship $d = 6/S \cdot \rho$, where S is the surface area per gram of ruthenium and ρ the density of ruthenium. The estimated average ruthenium particle size and the corresponding ruthenium dispersion (measured by PMR of the irreversible hydrogen with an assumed stoichiometric ratio of H(irr)/Ru(s) = 1) are listed in Table 2. Note that the average ruthenium particle size does not increase very much with an increase in the ruthenium loading.

The spin–lattice relaxation times of the hydrogen adsorbed on ruthenium and the silanol proton for all four ruthenium catalysts are also shown in Table 2. It is surprising to see a drastic decrease in the silanol group T_1 as the ruthenium loading increases. One may explain this by the increased iron impurity due to increasing ruthenium loading. No detectable iron was found in pure silica. The iron impurities originated mainly from the ruthenium salt $Ru(NO)(NO_3)_3$. Less than 8 ppm of iron was detected in the 12% Ru/SiO_2 catalyst by atomic absorption spectroscopy. Even though the iron may have induced relaxation of silanol group protons, it cannot fully account for such a large decrease in the spin–lattice relaxation time. Like the 4% Ru/SiO_2 catalyst, other ruthenium catalysts also exhibit a much longer T_1 of the silanol group proton when no hydrogen is dosed. It is therefore believed that the hydrogen adsorbed on ruthenium that has spilled over to the support is at least partially responsible for the sharp decrease in the spin–lattice relaxation time of the silanol proton.

On the basis of the measured iron content in the 12% ruthenium catalyst, we estimate that on the average each ruthenium particle (about 10,800 atoms) contains less than one Fe atom. If the trace amount of iron impurity is segregated to the surface of the ruthenium particles during reduction of the catalysts, as one may expect from the ther-

TABLE 2

Effects of Ruthenium Metal Loading

Ruthenium metal loading (wt%)	Average ruthenium particle size (nm), (dispersion)	Spin–lattice relaxation time T_1 (s)			
		Upfield peak		Downfield peak	
		5 Torr H_2	Strong H	5 Torr H_2	Strong H
1	3.4 (0.30)	0.019	0.024	18.3	19.2
4	3.9 (0.26)	0.021	0.026	3.2	5.4
8	4.3 (0.23)	0.029	0.031	1.0	1.5
12	5.3 (0.19)	0.043	0.044	0.7	1.1

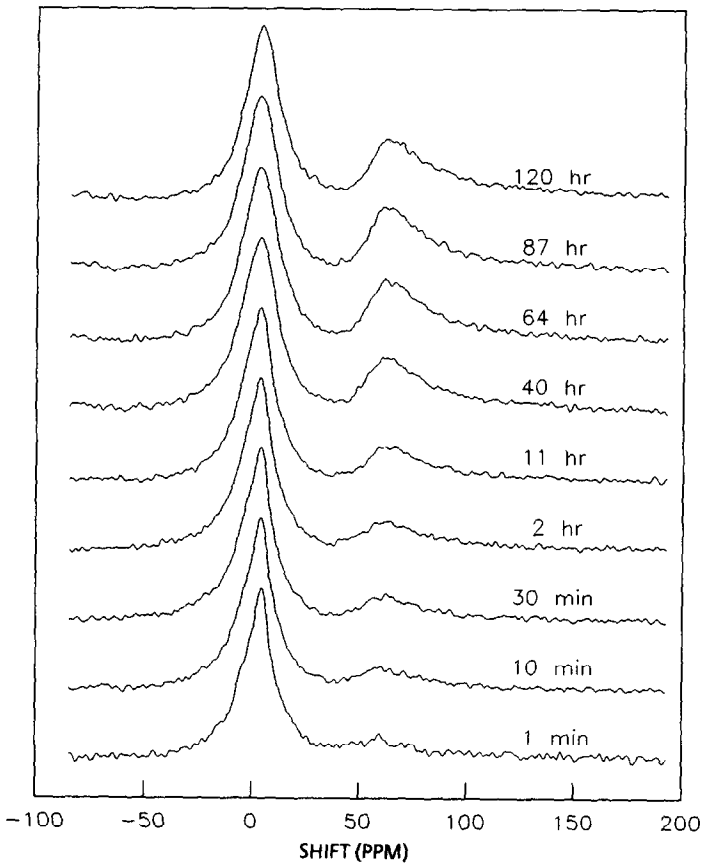

FIG. 8. PMR spectra on a 4% Ru/SiO_2 catalyst showing the progress of hydrogen–deuterium exchange with time at 294 K. The catalyst sample was initially under 5 Torr deuterium. Two hundred scans were accumulated for each spectrum.

modynamics of surface segregation, a decrease in T_1 of the adsorbed hydrogen on ruthenium with increase in ruthenium particle size should be observed due to increased surface concentration of iron. However, as shown in Table 2, the spin–lattice relaxation time of the adsorbed hydrogen on the surface of ruthenium increases with an increase in the ruthenium particle size. This result may indicate that the adsorbed hydrogen experiences many different structural environments on the surface of the ruthenium particles.

Figure 8 shows the PMR spectra, which indicate the progress of the hydrogen–deuterium exchange with time at ambient temperature on a 4% Ru/SiO_2 catalyst. The catalyst was under 5 Torr deuterium at the onset of the exchange experiment. Obviously, the exchange between the deuterium adsorbed on ruthenium (not detectable by PMR) and the silanol proton at room temperature is a very slow process. The half-life (with 50% deuterium exchanged) for the exchange process at 294 K is about 12 h. This is much shorter than that reported by Sheng and Gay (*20*). The reason for the discrepancy seems to be the residual chlorine present in the Ru/SiO_2 catalysts used by these researchers. If chlorine can inhibit adsorption of hydrogen on ruthenium, as mentioned earlier, it may slow the hydrogen–deuterium exchange as well.

As the upfield peak grows with time, the first moment of the upfield peak moves farther upfield. As shown earlier in Fig. 7, the

irreversible hydrogen on ruthenium has a smaller upfield shift than the reversible hydrogen. Therefore, this change of lineshift with time simply indicates that the exchanged hydrogen fills the ruthenium adsorption sites for the irreversible hydrogen first before covering sites for the reversible hydrogen.

Figure 9 shows the PMR spectra on a 4% Ru/SiO_2 catalyst which has been evacuated at 10^{-6} Torr for 10 min at room temperature after being dosed with 5 Torr deuterium at 77 K. In other words, only the irreversible deuterium is present on the surface of ruthenium; the reversible deuterium has been removed by evacuation. As shown in the figure, the initial intensity of the upfield peak is not observable and the peak does not grow with time, indicating the absence of hydrogen–deuterium exchange.

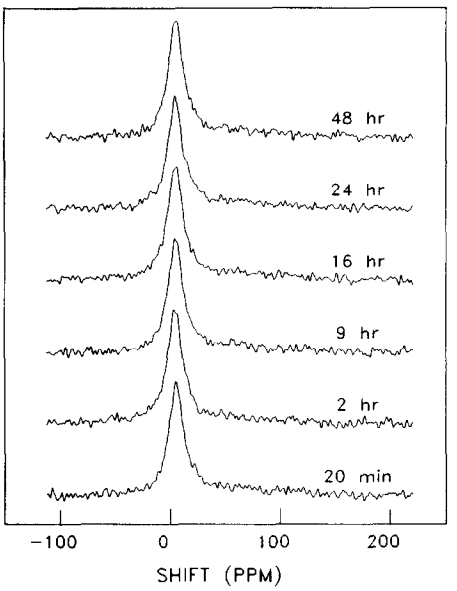

FIG. 9. PMR spectra on a 4% Ru/SiO_2 catalyst showing the absence of hydrogen–deuterium exchange at 294 K. The catalyst sample was exposed initially under 5 Torr deuterium at 77 K and was then evacuated to 10^{-6} Torr for 10 min at 294 K. Five hundred scans were accumulated for each spectrum.

DISCUSSION

Hydrogen Spillover

The present study indicates that there are two states of weakly adsorbed hydrogen in Ru/SiO_2 catalysts: (a) reversibly adsorbed hydrogen on ruthenium, and (b) spiltover hydrogen on the silica support. The amounts of these two states of hydrogen increases with increase in hydrogen pressure in the pressure range 0–30 Torr, especially that of reversible hydrogen on ruthenium. The reversible hydrogen on ruthenium and most of the spiltover hydrogen can be readily removed at room temperature under vacuum. The reversibility of adsorption for these two states of hydrogen and their dependence upon the hydrogen pressure indicate the existence of a dynamic equilibrium among the gas-phase hydrogen and these two states of weakly adsorbed hydrogen.

Evidence of hydrogen spillover has been presented by the increased discrepancy in counting hydrogen between the method of total hydrogen chemisorption and the PMR technique as the ruthenium loading is increased. While there are only moderate changes in the ruthenium particle size and dispersion, the total ruthenium surface area increases significantly with increase in the ruthenium loading. Therefore, hydrogen spillover is in some way related to the total available ruthenium surface area in the catalysts. As shown previously in Fig. 5, the amount of spiltover hydrogen increases with an increase in the total ruthenium surface area.

The noticeable changes in the lineshift and linewidth of the downfield peak (silanol group) with ruthenium loading as shown previously in Fig. 1 may also be an indication of hydrogen spillover. Since there are only two resonance lines observed, and the upfield resonance line is associated only with the Knight shift of adsorbed hydrogen on the surface of ruthenium, the line position of the spiltover hydrogen must be near that of the silanol group and its signal is buried under the large resonance line of the silanol group proton.

The effect of dosed hydrogen in shortening the spin–lattice relaxation time of the silanol group proton is obvious and convincing evidence of hydrogen spillover. Evacuation of the catalyst sample after dosing hydrogen does not return T_1 of the silanol group fully back to T_1 of a sample under vacuum without dosing hydrogen. This indicates that some of the spiltover hydrogen is not readily removed by evacuation and remains in the silica support. The sharp decrease in T_1 of the silanol proton with increase in ruthenium loading under the same treatment by hydrogen also points to the conclusion of hydrogen spillover. This is consistent with the fact that more spiltover hydrogen is present in catalysts with higher ruthenium loadings.

Although the nature of the spiltover hydrogen sites cannot be clearly identified by PMR, it is reasonable to postulate that the bridge oxygen (Si$\diagup$O$\diagdown$Si) in the silica support is responsible for holding the spiltover hydrogen. The spiltover hydrogen residing on the bridge oxygen is weakly bound and readily returns to the gas phase. Therefore, a constant supply of atomic hydrogen is required to maintain a measurable amount of spiltover hydrogen. The atomic hydrogen supply can only come from the hydrogen adsorbed on ruthenium. The spiltover hydrogen diffuses from the source to the bridge oxygen sites in the vicinity of the source; i.e., spiltover hydrogen populates only those sites that are near the ruthenium particles. Further diffusion of the spiltover hydrogen across the silica support may result in a recombination of the spiltover hydrogen to molecular hydrogen. This argument is supported by the fact that the amount of spiltover hydrogen increases as the total number of ruthenium particles or the total ruthenium surface area is increased. A recent PMR spin-labeling experiment performed on the Rh/SiO_2 catalyst indicates the existence of an unidentified hydrogen species in the immediate neighborhood of the Rh particles (*24*). This hydrogen species is likely to be the spiltover hydrogen.

Using the average ruthenium particle sizes listed in Table 2, we estimate the average distance between two ruthenium particles is to be about 1400 Å for the 1% Ru/SiO_2 catalyst and 880 Å for the 12% Ru/SiO_2 catalyst. As noted by Sheng and Gay (*18*) in their study on Pt/SiO_2 catalysts, the relaxation effect on silanol protons cannot be explained solely by spin diffusion due to dipolar T_2 processes originating near the metal particles and propagating such long distances. Thus the relaxation effect of the silanol proton can only be caused by the spiltover hydrogen. It is conceivable that T_1 of the spiltover hydrogen is very short, probably on the same order of magnitude as T_1 of the adsorbed hydrogen on ruthenium (~10 ms) or even shorter. This short T_1 may be due to weak bonding of the spiltover hydrogen atom to the bridge oxygen atom, which may have a strong relaxation effect. If the distribution of spiltover hydrogen in the silica support is such that most of the spiltover hydrogen is close to the ruthenium particle, then those silanol protons near the ruthenium particle are expected to relax much faster than those away from the ruthenium particle. As the total number of ruthenium particles and the total number of surface ruthenium atoms in the catalyst increase, the amount of spiltover hydrogen also increases. An increasing number of silanol protons would then experience the T_1 relaxation effect due to interaction with the spiltover hydrogen. One such possible interaction is through spin diffusion via dipolar T_2 processes among the spiltover hydrogen and the silanol proton. Another possible interaction may come from chemical exchange between the spiltover hydrogen and the silanol proton. But chemical exchange between the spiltover hydrogen and the silanol proton is much too slow compared to the observed T_1 of the silanol proton, as indicated by the result of the deuterium exchange experiment shown in Fig. 8. Therefore, the effect of chemical ex-

change on the T_1 of the silanol proton is insignificant at room temperature.

As can be seen in Fig. 5, both the amount of reversible hydrogen on ruthenium and the amount of spiltover hydrogen increase as the total amount of surface ruthenium is increased although they follow a different trend. It seems reasonable to suggest that the increase in the amount of spiltover hydrogen is caused by the increase in the amount of reversible hydrogen on ruthenium. Yet the different increasing trend also suggests variation in efficiency of hydrogen spiltover. Figure 10 shows the direct correlation between the spiltover hydrogen and the reversible hydrogen on ruthenium on a basis of per surface ruthenium atom. Clearly, hydrogen spillover is more efficient for ruthenium particles with lower dispersion, even though the fraction of reversible hydrogen per surface ruthenium atom is less. In other words, spiltover hydrogen coming off a larger ruthenium particle can diffuse farther onto the silica support. This result is consistent with the observations of narrower linewidth and longer T_1 for the reversible hydrogen on larger ruthenium particles. Such observations indicate a higher degree of mobility and weaker interaction with the surface ruthenium atoms.

Thermodynamics indicates that it is unlikely that the irreversibly adsorbed hydrogen on ruthenium would spill over to the silica support at room temperature. This would be a highly endothermic process, with an energy barrier of at least 16 kcal/mol (*25, 26*). However, hydrogen spillover from the reversibly adsorbed hydrogen on ruthenium to the silica support would seem to be energetically possible at room temperature. The reversibility of this adsorbed state of hydrogen on ruthenium indicates that there is little or no energy barrier that may prevent removal of this state of hydrogen from the surface of ruthenium.

Note that there is an absence of chemical exchange between the deuterium adsorbed on ruthenium and the silanol proton when the reversible deuterium is removed by evacuation, as indicated by Fig. 9. This observation confirms the notion that the irreversible hydrogen on ruthenium does not spill over onto the support. The present

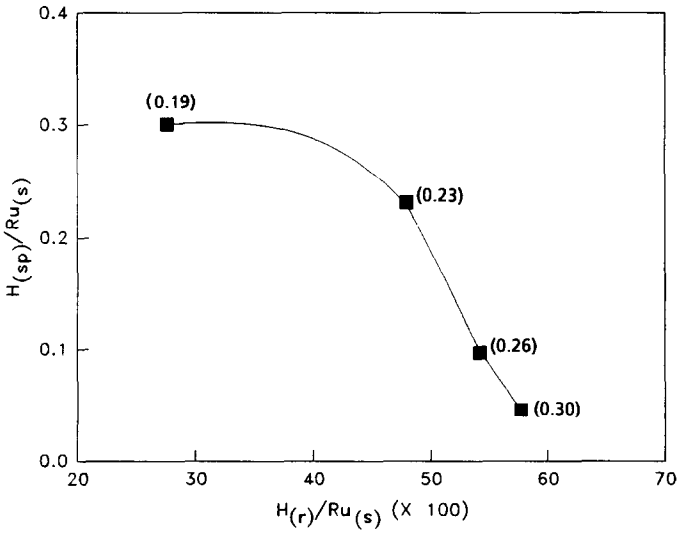

FIG. 10. Plot of spiltover hydrogen per surface ruthenium atom versus reversible hydrogen on ruthenium per surface ruthenium atom. The numbers in parenthesis are values of ruthenium dispersion calculated from PMR measurements of the irreversible hydrogen.

results indicate that chemical exchange between the reversibly adsorbed hydrogen on ruthenium and the silanol proton occurs via the spiltover hydrogen that acts as an intermediate for the exchange.

In the case of a hydrogen–deuterium exchange, some of the silanol protons are replaced by the incoming spiltover deuterium and become spiltover hydrogen, which, in turn, migrates back to a ruthenium particle and appears as reversibly adsorbed hydrogen. As indicated by the set of spectra in Fig. 8, the reversibly adsorbed hydrogen will replace the irreversibly adsorbed deuterium and become irreversibly adsorbed. The process continues until the surface of ruthenium is saturated with both adsorbed states of hydrogen.

Hydrogen Adsorbed on Ruthenium

The mobility of the reversible hydrogen on ruthenium is evident from the linewidth of its resonance spectrum, as shown previously in Fig. 6. Of all the catalysts investigated in this study, the linewidth of the resonance corresponding to the irreversible hydrogen on ruthenium is always 4–6 kHz wider than that corresponding to the reversible hydrogen on ruthenium. In other words, motional averaging of internal interactions between atoms of the reversible hydrogen on ruthenium reduces the resonance linewidth by about 5 kHz relative to that of strongly bound species. If the line broadening of the resonance of hydrogen adsorbed on ruthenium arises from the combined effects of H–H dipolar interactions, chemical shift anisotropy, and magnetic susceptibility broadening, then fast motion should at least average some of the broadening due to dipolar interactions and chemical shift anisotropy.

The variation of the upfield peak shift with the ruthenium loading (also the dispersion) shown in Fig. 7 may be due both to the effect of different ruthenium adsorption sites and to magnetic susceptibility variations arising from change in the ruthenium particle size. The effect of different ruthenium adsorption sites can be clearly seen in the results of T_1 on the adsorbed hydrogen (Table 2). The trend to longer T_1 of the adsorbed hydrogen with increase in ruthenium particle size (or decrease in dispersion) indicates a weaker interaction between the adsorbed hydrogen and the ruthenium adsorption sites. The adsorption sites may be categorized into two types: (I) surface ruthenium atoms on low index planes of the crystallite, much like those in ruthenium single crystals; and (II) surface ruthenium atoms on edges and corners or around defect structures, which are less fully coordinated atoms than the first type. As the ruthenium dispersion increases, the fraction of Type II ruthenium atoms increases. If T_1 of the adsorbed hydrogen on Type II ruthenium atoms is much shorter than that on Type I ruthenium atoms, then the observed trend in T_1 can be easily explained. In addition, if the lineshift of the adsorbed hydrogen on Type II ruthenium atoms is farther upfield than that on Type I ruthenium atoms, the observed shift variation may also be explained. However, to what extent the magnetic susceptibility of ruthenium particles may influence the shift of the adsorbed hydrogen cannot be determined in the present study. But, since the change in ruthenium particle size with ruthenium loading is moderate, the effect of magnetic susceptibility may be of secondary importance.

The ratio of the reversible hydrogen to surface ruthenium, as a function of the ruthenium dispersion, is shown in Fig. 11. This ratio is the difference between the total H/Ru and the irreversible H/Ru measured by PMR divided by the ruthenium dispersion as measured by PMR of irreversibly adsorbed hydrogen. The trend to larger $H_{(r)}/Ru_{(s)}$ with increase in dispersion is an indication that the reversible hydrogen is at least in part associated with Type II ruthenium atoms. Some of the reversible hydrogen is also associated with Type I ruthenium atoms since $H_{(r)}/Ru_{(s)}$ for a clean ruthenium powder (~0.3) is about the same

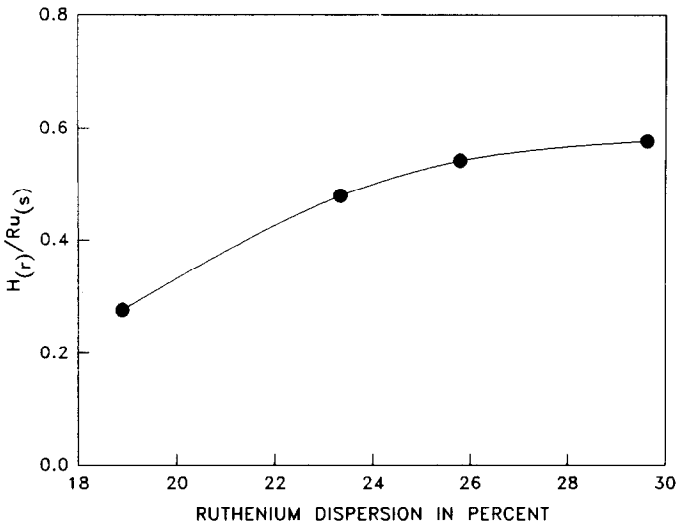

FIG. 11. Plot of the ratio of reversible hydrogen on ruthenium to surface ruthenium versus ruthenium dispersion. The amount of reversible hydrogen is measured by PMR. Ruthenium dispersion is calculated from the amount of irreversible hydrogen measured by PMR.

as that for the 12% ruthenium catalyst as measured by the volumetric technique. It is reasonable to conceive that the irreversible hydrogen sits in threefold hollow sites among Type I ruthenium atoms and is relatively less mobile while the reversible hydrogen moves freely on top of surface ruthenium atoms. For the Type II ruthenium atoms, multiple hydrogen adsorption is possible because they are less fully coordinated. In this case, one irreversible hydrogen and one or more reversible hydrogen can be adsorbed on the same site.

CONCLUSIONS

Hydrogen adsorption on Ru/SiO_2 catalysts at ambient temperature generates two adsorbed states of hydrogen on ruthenium, irreversible hydrogen and reversible hydrogen, and two states of hydrogen on SiO_2, spiltover hydrogen and physisorbed hydrogen. The physisorbed hydrogen is of minor importance. The reversible hydrogen on ruthenium is the source of hydrogen spillover. Both the reversible hydrogen and the spiltover hydrogen introduce errors in determining the ruthenium dispersion by the traditional volumetric method. Measurements of the irreversible hydrogen by both PMR and hydrogen chemisorption are in good agreement. The amount of the irreversible hydrogen would appear to be appropriate to use in determination of ruthenium dispersion.

From PMR it is inferred that the reversible hydrogen on ruthenium is much more mobile at room temperature than the irreversible hydrogen. Multiple hydrogen adsorption on ruthenium is suggested for catalysts with high dispersion. At least two different types of ruthenium adsorption sites exist on the surface of ruthenium particles: sites with low index planes and sites with defect-like structures. The relative distribution of these two types of adsorption sites varies with the ruthenium dispersion. Sites with a lower ruthenium coordination interact more strongly with the adsorbed hydrogen, perhaps due to variations in local valence electron density.

ACKNOWLEDGMENT

This work was supported by the U.S. Department of Energy, Office of Basic Energy Sciences, Contract W-7405-ENG-82.

REFERENCES

1. Dalla Betta, R. A., *J. Catal.* **34,** 57 (1974).
2. Kubicka, H., *J. Catal.* **12,** 233 (1968).
3. Sinfelt, J. H., and Yates, D. J. C., *J. Catal.* **8,** 82 (1967).
4. Gay, I. D., *J. Catal.* **80,** 231 (1983).
5. Taylor, K. C., *J. Catal.* **38,** 299 (1975).
6. Goodwin, J. G., Jr., *J. Catal.* **68,** 227 (1981).
7. Yang, C. H., and Goodwin, J. G., Jr., *J. Catal.* **78,** 182 (1982).
8. Chen, Y. W., Wang, H. T., and Goodwin, J. G., Jr., *J. Catal.* **83,** 415 (1983).
9. Sinfelt, J. H., Lam, Y. L., Cusumano, J. A., and Barnett, A. E., *J. Catal.* **42,** 227 (1976).
10. Rouco, A. J., Haller, G. L., Oliver, J. A., and Kemball, C., *J. Catal.* **84,** 297 (1983).
11. Sermon, P. A., and Bond, G. C., *Catal. Rev.* **8,** 211 (1973).
12. Conner, W. C., Jr., Pajonk, G. M., and Teichner, S. J., *in* "Advances in Catalysis" (D. D. Eley, P. W. Selwood, and Paul B. Weisz, Eds.), Vol. 34, p. 1. Academic Press, New York, 1985.
13. Narita, T., Miura, H., Sugiyama, K., Matsuda, T., and Gonzalez, R. D., *J. Catal.* **103,** 492 (1987).
14. Narita, T., Miura, H., Sugiyama, K., Matsuda, T., and Gonzalez, R. D., *Appl. Catal.* **32,** 185 (1987).
15. Lu, K., and Tatarchuk, B. J., *J. Catal.* **106,** 166 (1987).
16. Lu, K., and Tatarchuk, B. J., *J. Catal.* **106,** 176 (1987).
17. De Menorval, L. C., and Fraissard, J. P., *Chem. Phys. Lett.* **77,** 309 (1981).
18. Sheng, T. C., and Gay, I. D., *J. Catal.* **71,** 119 (1981).
19. Sheng, T. C., and Gay, I. D., *J. Catal.* **77,** 53 (1982).
20. King, T. S., Wu, X., and Gerstein, B. C., *J. Amer. Chem. Soc.* **108,** 6056 (1986).
21. Wu, X., Gerstein, B. C., and King, T. S., submitted for publication.
22. Cheung, T. T. P., Worthington, L. E., Murphy, P. D. B., and Gerstein, B. C., *J. Magn. Reson.* **41,** 158 (1980).
23. Sanz, J., and Rojo, J. M., *J. Phys. Chem.* **89,** 4974 (1985).
24. Root, T. W., and Duncan, T. M., *Chem. Phys. Lett.* **137,** 57 (1987).
25. Shimizu, H., Christmann, K., and Ertl, G., *J. Catal.* **61,** 412 (1980).
26. Feulner, P., and Menzel, D., *Surf. Sci.* **154,** 465 (1985).